Fission fragment mass distribution in the ^{28}Si + ^{144}Sm reaction

T. N. Nag[1,3*], R. Tripathi[1,3], S. Sodaye[1,3], S. Santra[2,3], P. C. Rout[2,3], K. Mahata[2,3], K. Ramachandran[2], S. Gupta[2], A. Shrivastava[2,3] and P. K. Pujari[1,3]

[1]*Radiochemistry Division, Bhabha Atomic Research Centre, Mumbai - 400085, INDIA*
[2]*Nuclear Physics Division, Bhabha Atomic Research Centre, Mumbai - 400085, INDIA*
[3]*Homi Bhabha National Institute, Anushaktinagar, Mumbai-400094, INDIA*
**email: tarak@barc.gov.in*

Introduction

Investigation of fission fragment mass distribution for the fissioning systems in the sub-lead region are important topic of research in the recent days. Observation of asymmetric mass distribution in beta-delayed fission of (βDF) ^{180}Tl has driven a renewed interest on the fission fragment mass distribution in ^{180}Hg as conventional theory of nuclear shell model predicts symmetric mass distribution leading to two ^{90}Zr having semi magic configuration with N = 50, Z = 40 [1]. Various theoretical and experimental investigations have been carried out to understand this unexpected observation [2,3]. Theoretical calculations by Moller *et al.* suggested that the observed mass asymmetry in ^{180}Hg is due to the pronounced single particle effects in the fissioning system [2]. The authors also showed that the asymmetric mass distribution is not only restricted to the ^{180}Hg but

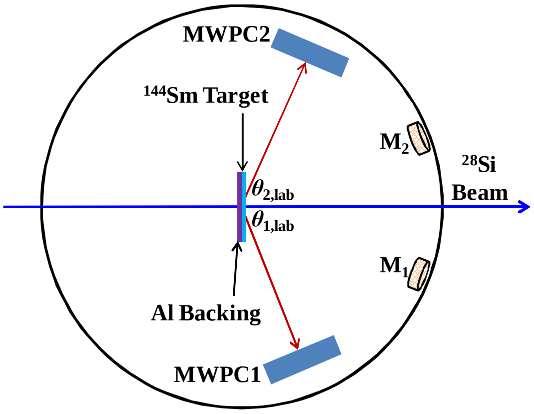

Fig. 1 *Schematic of detector setup for the ^{28}Si + ^{144}Sm reaction.*

also it could be expected for many other nuclei around the mass region $A \approx 180$ [2]. The flat-top mass distributions observed in various experimental studies for the fissioning system around the mass region $A \approx 180$ indicated the contribution from symmetric as well as asymmetric fission [3-5]. Recent theoretical calculations based on quadrupole and octupole deformation in the pre-formed fragments suggested that the observed asymmetry in the sub-lead region is due to the appearance of shell closure in the fragments with neutron no. $N \approx 52$, 56 and proton no. $Z \approx 34$, 44 and 52 [6]. K. Mahata *et al.* extended these calculations for many other systems and suggested that proton shell closure is the dominant drive force as compared to the neutron shell closure in observation of asymmetric mass distribution in the mass region $A \approx 180$ [7]. Various experimental studies of fission mass distributions have been carried out in order to investigate the mechanism of fission around the mass region $A > 176$ [3-5,8], however in the lighter mass region the mass distribution measurements are limited. Thus it is important explore the mass distribution measurements in the lighter mass region also.

With an objective to investigate the mechanism of fission, mass distribution measurements have been carried out in the sub-lead region in ^{172}Os compound nucleus, which was produced in ^{28}Si + ^{144}Sm reaction at beam energies $E_{\mathrm{lab}} \approx$ 124.3, 128.9 and 137.5 MeV corresponding to the excitation energy of the compound nucleus (^{172}Os) as 37.9, 41.7 and 48.9 MeV respectively.

Experimental Details

Experiments were carried out at BARC-TIFR Pelletron LINAC facility at TIFR Mumbai India. An electro deposited target of ^{144}Sm (Thickness ≈ 120 μg/cm^2; enrichment: 94%) on Aluminum backing (Thickness: 550 μg/cm^2) facing the beam, was bombarded with ^{28}Si beam at energies $E_{\mathrm{Beam}} \approx$ 129.6, 134 and 142.5 MeV. After accounting the energy loss in the target beam energies on the target were calculated as $E_{\mathrm{lab}} \approx$

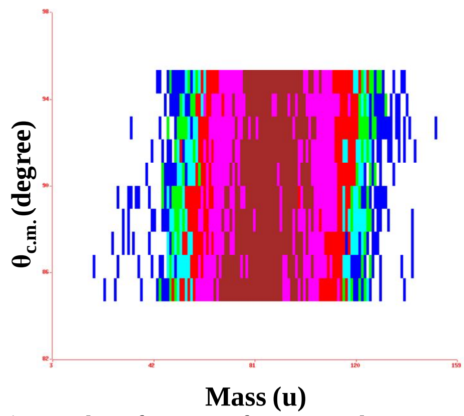

Fig. 2 *Plot of centre of mass angle versus Mass number of the fission fragments at 137.5 MeV.*

124.3, 128.9 and 137.5 MeV. Two multiwire proportional counters (MWPCs) were placed at ±68^0 in order to detect the two coincident fission fragments. The schematic of the detector set up is shown in Fig. 1. There are four positions and one timing signal for each MWPCs. The signals from each detector were fed in to a time to digital converter unit (TDC). The signals in the TDC were recorded by taking RF (beam pulse) as start signal. Stop signal was obtained, whenever a fission fragment was detected in either one of the counter. Two monitor detectors placed at ±20° were used to detect the elastically scattered beam particles.

Results and Discussions

In the present paper the mass distribution obtained at E_{lab} = 137.5 MeV is discussed. Determination of mass distribution was based on the time of flight (TOF) of the fission fragments. The electronic delay with respect to the beam pulse was obtained from the elastic peaks, which was used to calculate the TOF of the fission fragments. A further delay adjustment was required in order to make the parameter $V_{\|}/V_{\text{CN}}$ unity where $V_{\|}$ is the velocity of the fission system along the beam direction and V_{CN} is the recoil velocity of the compound nucleus. The energy loss of the fission fragments in the target was estimated using the prescription described in Refs. [3,9], and it was observed to be ≈ 3.5 MeV. Figure 2 shows the plot for $\theta_{\text{c.m.}}$ versus mass of the fission fragments. The events showed in the Fig. 2 are considered within

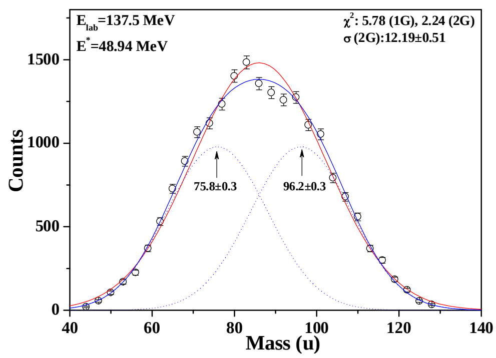

***Fig. 3** Mass distribution in $^{28}Si+^{144}Sm$ reaction at E_{lab}=137.5 MeV (E* = 48.9 MeV).*

the angle range 85°-95° in order to avoid the detector edge effect. A "X" axis projection of the Fig. 2 gives the mass distribution which is shown in Fig. 3. The mass distribution showed in Fig. 3 has pronounced flatness at symmetry indicating the contribution from multimodal fission. The nature of the mass distribution in the present study is similar to our earlier studies as observed in ^{35}Cl+^{144}Sm [4] and ^{32}S+^{144}Sm [3] reaction in similar excitation energy of the compound nucleus. It is evident from Fig. 3 that experimental mass distribution has two shoulders at A ≈ 96 and A ≈ 76, which further confirms the contribution from symmetric and asymmetric fission. Experimental mass distribution data have been tried to fit by both single-Gaussian (1G) and two-Gaussian (2G) function, which is shown in Fig. 3 as red and blue line for single and two Gaussian fit respectively, to the experimental data. The better fit was obtained with two Gaussian functions as evident from the improved chi-square value indicating the dominant contribution from asymmetric fission. The peak positions for the lighter and heavy mass wings are also mentioned in the Fig. 3 which was obtained from the two-Gaussian fit to the experimental data. The most probable neutron and proton number of the fragments were determined assuming the similar A/Z ratio of the fragments and the compound nucleus. The neutron no. for the heavy fragments and the proton no. for the lighter fragments were observed as N_{H} ≈ 52 and Z_{L} ≈ 34 respectively. This observation is consistent with the prediction from Refs. [6,7]. The calculated proton no. for the lighter fragment is found to be similar as observed in the earlier studies in the fissioning system mass range A ≈ 176-184. This observation further confirms the dominant role of proton shell closure in observing the asymmetric mass distribution of the fissioning system in the sub-lead region.

Conclusions

Fission fragment mass distribution has been determined in ^{28}Si + ^{144}Sm reaction at beam energies E_{lab} ≈ 124.3, 128.9 and 137.5 MeV. The analysis for the mass distribution data for E_{lab} = 137.5 MeV is presented here. The flatness in mass distribution in the symmetric region and shoulders around mass A ≈ 76 and ≈ 96 indicate the contribution from symmetric and asymmetric fission modes, which was further confirmed by the improved chi-square value in two-Gaussian fit to the experimental data as compared to the single Gaussian fit. Determination of neutron and proton no. in the fragments showed that the results are consistent with the theoretical prediction.

References

1. Andreyev *et al*., Phys. Rev. Lett. **105**, 252502 (2010).
2. Moller *et al*., Phys. Rev. C **85**, 024306 (2012).
3. T. N. Nag *et al*., Phys. Rev. C **103**, 034612 (2021).
4. R. Tripathi *et al.*, Phys. Rev. C **92**, 024610 (2015).
5. E. Prasad *et al*., Phys. Lett. B **811**, 135941 (2020).
6. G. Scamps *et al*., Phys. Rev. C **100**, 041602 (R) (2019).
7. K. Mahata *et al*., arXiv:2007.16184.
8. I. Tsekhanovich *et al*., Phys. Lett. B **790**, 583 (2019).
9. Hans-Dieter Betz *et al.*, Rev. Of Modern Phys. **44**, 3 (1972).